*Int. J. Electrochem. Sci.*, 10 **(2015)** 9073 - 9088

International Journal of
ELECTROCHEMICAL
SCIENCE
www.electrochemsci.org

# Cerium-based Chemical Conversion Coating on Aluminum Alloy to Inhibits Corrosion in Chloride Solution

*Siyi Chen, Shengtao Zhang*[*]*, Xiaolei Ren, Shenying Xu, Linliang Yin*

School of Chemistry and Chemical Engineering, Chongqing University, Chongqing 400044, P.R. China
[*]E-mail: Zhangstchongqing@163.com

*Received:* 15 July 2015 / *Accepted:* 21 August 2015 / *Published:* 30 September 2015

Chemical conversion coatings with rare-earth metal salts are being considered as an environment-friendly alternative to the toxic chromium-based coating to improve the corrosion resistance of aluminum alloy. However, the effects of conversion conditions on the coating performance are rarely systematically studied. In this study, we prepared the cerium-based conversion coatings on the ADC12 aluminum alloy in $Ce(NO_3)_3$ solution under different conversion conditions, including the additive ($H_2O_2$) concentration, the immersion time, the bath temperature, etc.. Then, the corrosion behavior of each cerium-coated sample was evaluated in 3%NaCl solution by the methods of potentiodynamic polarization, electrochemical impedance spectroscopy and surface observation technique techniques. The results reveal the corrosion resistance of Ce-based coatings on Aluminum alloy could be improved with increasing the concentration of additive, the immersion time and/or the bath temperature before reaching the best performance, but it will decrease if the conditions above exceed their corresponding optimal value. We believe the performance decrease after best performance is due to the cracks induced in thick coatings for higher concentration of additive or longer immersion time. As for the bath temperature, we believe the decrease is attributed to the decomposition of $H_2O_2$ in high temperature.

**Keywords:** Aluminum alloy, Cerium-based coating, Conversion condition, Corrosion resistance

## 1. INTRODUCTION

Aluminum and its alloys are common lightweight materials which are extensively applied in structural engineering due to its excellent mechanical property and anti-corrosion performance. Due to the highly reactivity of aluminum, a thin film of aluminum oxide ($Al_2O_3$) could form on the alloy surface in moist environment, which protect the underneath substrate from attacking to some extent. However, the potential difference between aluminum matrix and other alloy elements would result in

the occurrence of galvanic corrosion reaction in aggressive solution, especially with the presence of chloride ions ($Cl^-$), which shorten its service time significantly[1-7].

Traditional strategy for surface treatment to protect aluminum alloy is the hexavalent chromate conversion coating method, which is also successfully applied for other metals and alloys[8-11]. However, the high carcinogenicity and genotoxicity of this method has limited its applications in many countries. Therefore, some rare earth salts are being employed to develop alternative environment-friendly method to inhibit the corrosion protection of alloys. For example, cerium salts have been explored as corrosion inhibitors on aluminum and zinc[12], which formed a barrier coating on the metal surface to suppress the cathodic reaction. The conversion coatings were more resistant than the native oxide film, which could effectively inhibit the corrosion reaction on the metal surface. Such surface coatings are usually prepared via the methods of chemical conversion or electrochemical deposition after immersing the specimens into the conversion solution. And its corrosion protection performance depends on the properties of rare earth oxide/hydroxide film on the metal surface, which will be significantly affected by the conversion conditions, including solution components, bath temperature, immersion time, etc.. Besides, some additives[13-15], e.g. $H_2O_2$, are also supplemented into the conversion solution to accelerate the preparation process. Although various rare earth salts based conversion coatings has been developed in recent years[16-20], the effect of each conversion condition on the coating properties is rarely systematically studied. Additionally, how the additives affect the conversion reaction on the metal surface is still unclear.

In this paper, a $Ce(NO_3)_3$-$H_2O_2$ based solution is applied to prepare the chemical conversion coatings ADC12 aluminum alloys. The Ce-based coatings on aluminum alloy are prepared under different conversion conditions at first. And then, we conducted the measurements of Tafel polarization curves and electrochemical impedance spectroscopy (EIS) to evaluate the electrochemical property of conversion coating for each specimen, and to obtain the optimal conversion conditions of Ce-based coatings on aluminum alloy, i.e. temperature, immersion time, and $H_2O_2$ concentration. Based on such experiments, we aim to clarify the effect of additives, as well as conversion conditions, on the property of coatings on metal surface, and also set guidelines for coating preparation in the future.

## 2. EXPERIMENTAL

### *2.1 Materials*

The substrate material was ADC12 aluminum alloy, whose major chemical composition was listed in Table 1.

**Table 1** Major chemical composition of ADC12 aluminum alloy (% by mass)

| Alloy | Cu | Si | Mg | Zn | Fe | Mn | Ni | Sn | Al |
|---|---|---|---|---|---|---|---|---|---|
| ADC12 | 1.5-3.5 | 9.6-12.0 | ≤0.3 | ≤1.0 | ≤0.9 | ≤0.5 | ≤0.5 | ≤0.3 | balance |

*2.2 Formation of the cerium conversion coatings*

The alloy samples were cut into 1cm×1cm×1cm from the material received, then the specimens are embedded in epoxy resin with a geometrical surface area of 1cm$^2$ exposed to the electrolyte.

In present work, the Ce-based coating process are prepared as following steps successively: the samples are abraded with emery paper from 800 to 2000 grit →wiped with acetone →rinsed with deionized water →degreased ultrasonically in ethanol → rinsed with deionized water → cleaned with $HNO_3$ solution with pH value of 2 → rinsed with deionized water →dried with air →immersed into Ce salts baths for treatment→ rinsed with deionized water →dried at room temperature.

The cerium conversion baths contained a 5g/L $Ce(NO_3)_3 \cdot 6H_2O$ with different concentrations of $H_2O_2$, 40mL-120mL. The immersion time varied between 5 and 40 minutes, and the temperature ranged from 10 and 35℃ for conversion reaction. The pH value of each conversion solution was adjusted to around 2.8 with addition of $HNO_3$. After treatment, the coated samples were rinsed with deionized water and finally dried at room temperature. All the reagents used were of analytic grade, and the solutions were open to the air.

*2.3 Electrochemical experiment*

The corrosion behavior of each specimen was evaluated in 3%NaCl using the electrochemical experiment after treatment in corresponding conversion solution. The electrochemical measurements are conducted in a conventional three-electrode cell system. A freshly polished aluminum alloy specimen and a platinum electrode are used as working electrode (WE) and counter electrode (CE), respectively. And the CE surface area was at least two orders of magnitude larger than that of the WE. A saturated calomel electrode (SCE) with a Luggin capillary is used as reference electrode (RE). All potentials are measured versus SCE and tests are performed in non-deaerated solution, and all measurements were carried out at room temperature. Electrochemical impedance spectroscopy (EIS) measurements are carried out at the open circuit potential (OCP). The ac frequency range extends from 100kHz to 10mHz with a 5mV peak-to-peak sine wave as the excitation signal. The impedance data are analyzed and fitted with ZsimpWin. The potentiodynamic electrochemical polarization curves are obtained from -250 to +250 mV (versus OCP) with 2 mV/s scan rate, and the data are collected and analyzed by electrochemical software PowerSuite ver. 2.58. Each experiment were repeated at least three time to check the reproducibility.

*2.4 Morphological characterization and composition determination*

The microstructure of the conversion coatings was determined with scanning electron microscopy (SEM). And its chemical components were determined with energy dispersion X-ray spectroscopy (EDS) whose detector was connected to the SEM-device. The contact angles (CA) on the bare aluminum alloy and those on the alloy treated in $Ce(NO_3)_3$ solution and $Ce(NO_3)_3$-$H_2O_2$ solution were measured by the sessile water drop method by a contact angle goniometer (Dataphysics OCA20,

Germany). The average contact angles value was obtained by more than three valid measurements on different spots of the same sample.

## 3. RESULTS AND DISCUSSION

### *3.1 contact angle measurements*

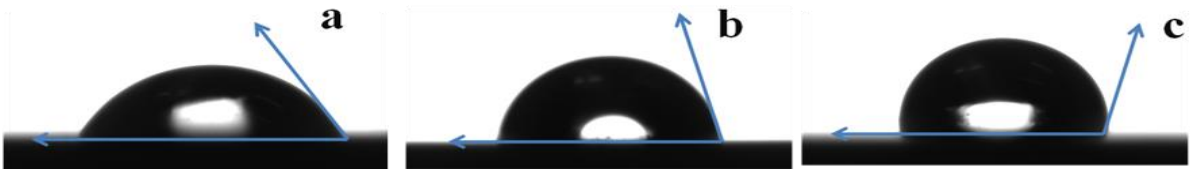


**Figure 1.** Sessile water drop images on: (a) Bare aluminum alloy; (b) The sample treated in $Ce(NO_3)_3$ solution; (c) The sample treated in $Ce(NO_3)_3$-$H_2O_2$ solution.

The wettability of cerium-based coatings was examined by measuring the contact angle. The images of the sessile water drop on the bare aluminum alloy and those on the samples after treatment in cerium salt solution with and without $H_2O_2$ are shown in Fig.1a-b, respectively. We can observe that the bare aluminum alloy has a hydrophilic surface for the contact angle of approximately 66.6°(Fig. 1 c), whereas the angle on the sample treated with only $Ce(NO_3)_3$ solution is 86.7°(Fig. 1b), and the one with $Ce(NO_3)_3$-$H_2O_2$ solution is 102.4°(Fig. 1a). Generally, the value of contact angle mainly depends on the properties of coatings, and the larger value indicates better hydrophobic ability and more uniform surface on the aluminum alloy, which enhances the corrosion resistance of coatings. It is obvious that the contact angles significantly increase after the cerium conversion treatment, suggesting the formation of a hydrophobic film. Moreover, we can also find that the treatment with additive exhibits better surface hydrophobicity than the one without, indicating the additive of $H_2O_2$ could improve the coating performance.

### *3.2 Superficial morphology*

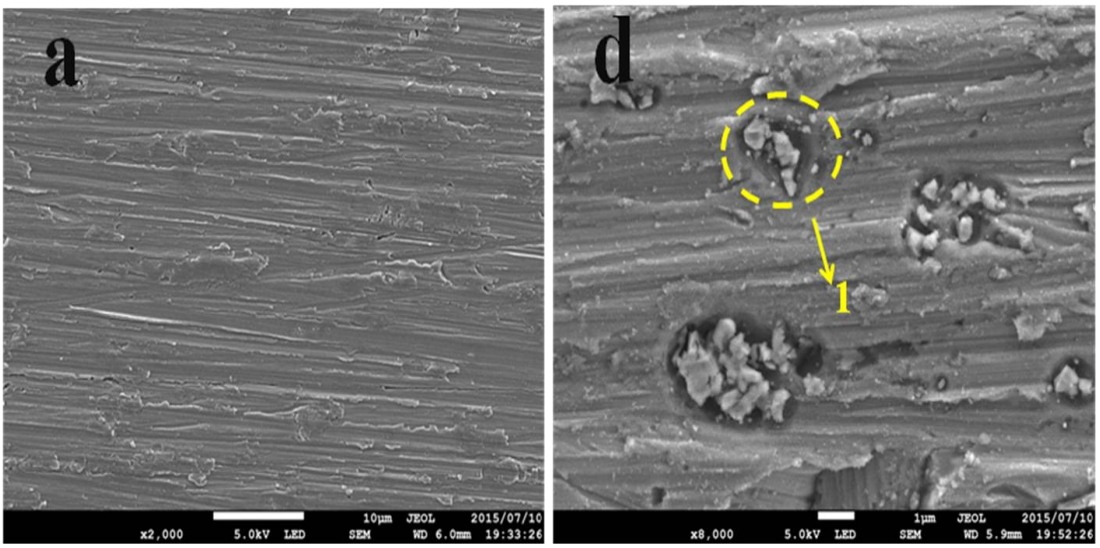

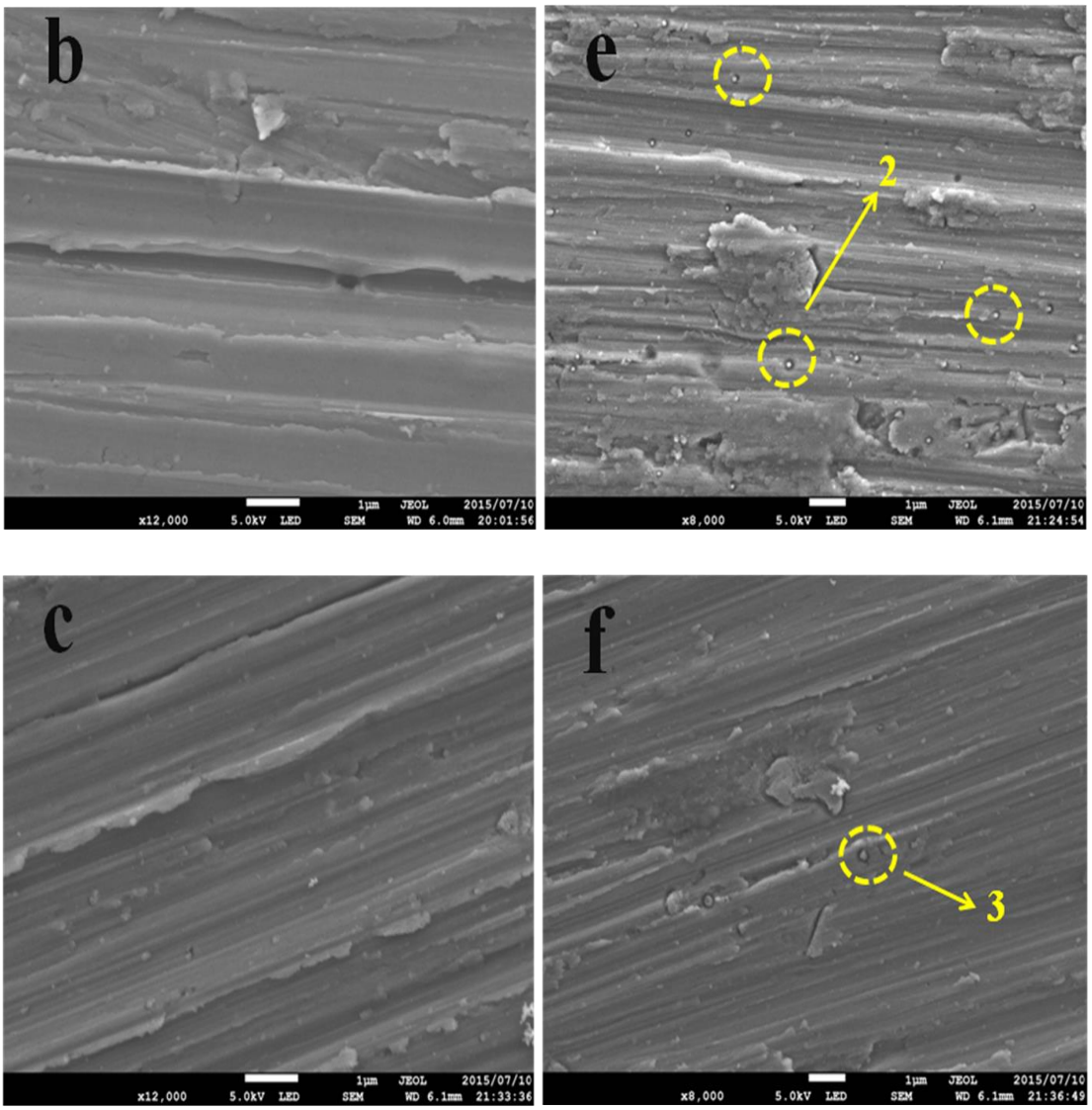


**Figure 2.** SEM micrographs of the cerium conversion coatings before and after 1h immersion in 3%NaCl solution: (a, d) Bare aluminum alloy; (b, e) The coating treated in $Ce(NO_3)_3$ solution; (c, f) The coating treated in $Ce(NO_3)_3$-$H_2O_2$ solution.

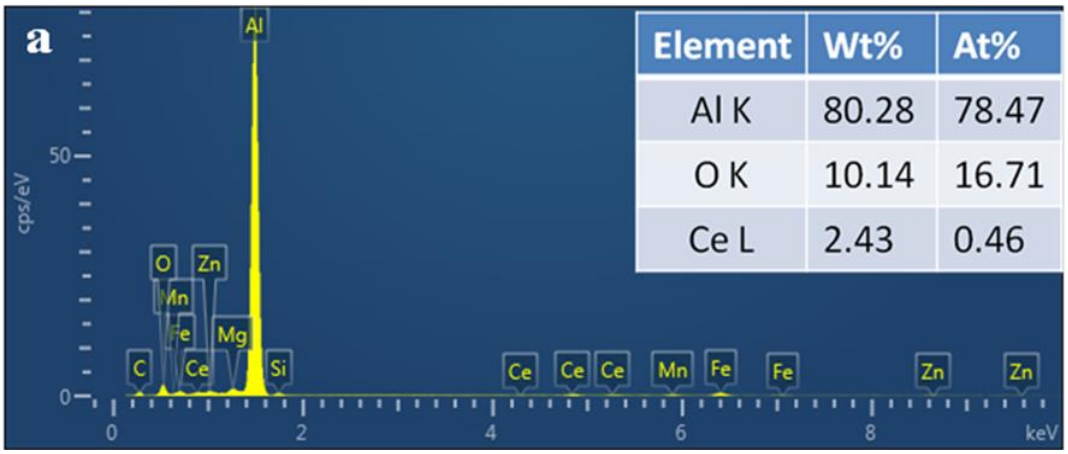


| Element | Wt% | At% |
|---|---|---|
| Al K | 80.28 | 78.47 |
| O K | 10.14 | 16.71 |
| Ce L | 2.43 | 0.46 |

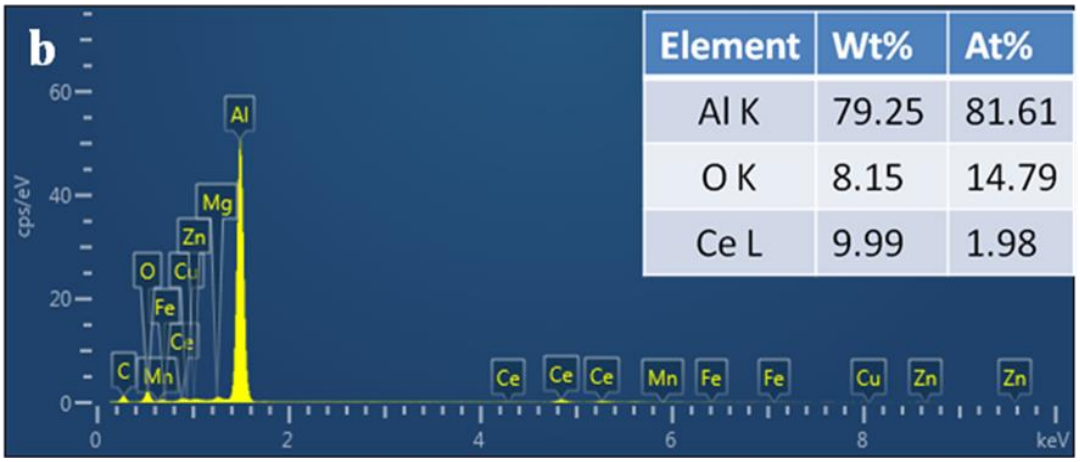


**Figure 3.** EDS spectra acquired on aluminum alloy samples after (a) treating in $Ce(NO_3)_3$ aerated aqueous solution; and (b) treating in $Ce(NO_3)_3$-$H_2O_2$ solution.

Surface images of two kinds of cerium conversion coatings on ADC12 aluminum alloy before and after 1h immersion in 3%NaCl solution are presented in Fig. 2. Fig. 2a is the untreated surface of aluminum alloy as a reference.

As observed, when additive ($H_2O_2$) is added into the cerium conversion solution, the coating surface appears to be more uniform and smoother than that formed without additive, as shown in Fig. 2b-c. Micrographs in Fig. 2 show that destroy of Ce-based coating in NaCl solution is initiated with pitting corrosion. More pits (designated by "2") are observed on the surface of the sample treated in cerium nitrate solution and few pits (designated by "3") are observed on the surface of the one treated in additive after 1h immersion in 3%NaCl solution. Thus, we can conclude that the coating treated in $Ce(NO_3)_3$-$H_2O_2$ solution produced more resistant surface than that of the one treated without $H_2O_2$.

Fig. 3 show the EDS plane-scanning spectra curves for elements corresponding to Ce conversion coatings (X-axis is element's character energy and Y-axis is count for it). The EDS analysis reveals that the surface treated in $Ce(NO_3)_3$-$H_2O_2$ solution contains higher cerium content. Such result confirms that the additive of H2O2 could remarkably increases the cerium content in the coating, which might because $H_2O_2$ can accelerate the conversion reaction during the coating formation process.

### *3.3 Electrochemical analysis*

#### *3.3.1 The effect of $H_2O_2$ concentration*

As reported[21], the conversion coatings result from the deposition of insoluble rare-earth salts with the increase of local pH by cathodic reaction, which can be catalyzed with the additive of $H_2O_2$. However, it is still unclear that how the concentration of $H_2O_2$ in the conversion solution affects the coating performance. Thus, we prepared the Ce-based coating on aluminum alloy specimens in conversion solution with different concentrations of $H_2O_2$, and then, evaluated the electrochemical behaviors of each specimen in 3% NaCl solution, as shown in Fig.4. Table 2 lists the corrosion

parameters including corrosion potential ($E_{corr}$), corrosion current density ($I_{corr}$), and Tafel slope ($\beta_a$ , $\beta_c$). The $E_{corr}$ and $I_{corr}$ were determined by extrapolation of the cathodic and anodic Tafel regions in the polarization curves. In order to evaluate the performance of Ce-based coatings on aluminum alloy, the protective efficiency, IE(%), was calculated using the following equation:

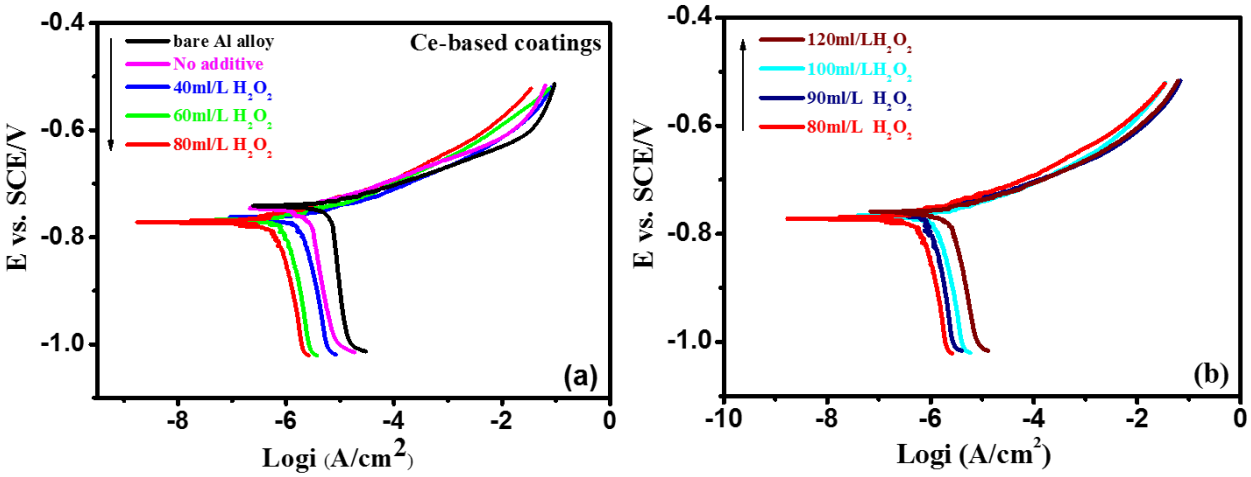


**Figure 4.** Potentiodynamic polarization curves of cerium-coated Al alloy in 3% NaCl solution. (a) The effect of $H_2O_2$ concentration on polarization curves below 80ml/L; (b) The effect of $H_2O_2$ concentration on polarization curves above 80ml/L; ($Ce(NO_3)_3$=5g/L, T =25℃, t =20min).

**Table 2** Potentiodynamic polarization parameters for the corrosion of Cerium-coated aluminum alloy in 3% NaCl solution after being treated in conversion solution with different concentration of $H_2O_2$.

| $H_2O_2$ Concentration | $E_{corr}$ (mV/SCE) | $\beta_c$ (mV · $dec^{-1}$) | $\beta_a$ (mV · $dec^{-1}$) | $I_{corr}$ (μA · $cm^{-2}$) | IE (%) |
|---|---|---|---|---|---|
| Blank | -741 | 907.44 | 32.81 | 9.409 | — |
| No additives | -746 | 584.80 | 33.07 | 4.004 | 57.44% |
| 40ml/L | -763 | 415.28 | 27.75 | 2.459 | 73.87% |
| 60ml/L | -768 | 394.32 | 29.99 | 1.079 | 88.53% |
| 80ml/L | -772 | 389.26 | 37.04 | 0.562 | 94.03% |
| 90ml/L | -763 | 388.05 | 27.99 | 1.367 | 85.47% |
| 100ml/L | -766 | 388.65 | 29.81 | 2.140 | 77.26% |
| 120ml/L | -759 | 413.74 | 31.30 | 2.796 | 70.28% |

$$IE(\%) = \frac{i_{corr}^0 - i_{corr}}{i_{corr}^0} \times 100\% \qquad (1)$$

Where $i_{corr}^{o}$ and $i_{corr}$ are the corrosion current density of aluminum alloy without and Ce-based coatings, respectively.

The effect of additive ($H_2O_2$) concentration on the corrosion behavior of Ce-based coatings surface is depicted in Fig.4a-b. It is obvious that all the polarization curves of aluminum alloy specimens treated in the conversion solution with $H_2O_2$ exhibit lower corrosion current density and more negatively corrosion potential than the one without, suggesting the additive of $H_2O_2$ enhance the protection performance of Ce-based coating. As observed in Fig.4a-b, the specimens treated in the conversion solution with 80mL/L $H_2O_2$ exhibits the most negative corrosion potential (-772mV vs SCE), which decrease 26mV compared to the one treated in the solution without additive (-746mV vs SCE). According to Conde et al.[22], the negative shift of corrosion potential is attributed to the increase of area covered by insoluble cerium salts. Thus, the decrease of corrosion potential demonstrates the additive of $H_2O_2$ could promote the formation of conversion film on the aluminum alloy. However, as we further increase the concentration of additive to 120mL, the corrosion potential convert to increase direction and slightly positive shift to -759mV vs SCE. This is might because the deposition rate of insoluble cerium salts is too fast in the conversion solution with relative higher concentration of additive, which we will further explained below.

From the Fig.4, we can see that the cathodic branch remains the same trend for all the coated samples, which are toward lower current densities, corresponding to smaller cathodic slopes (βc). However, the anodic branch almost no move down. The effect on Tafel slopes may be due to many factors, such as electrode material, the composition of solution, temperature, and charge transfer coefficient. For aluminum alloy, corrosion is a combination of two electrochemical reactions involving anodic areas where aluminum dissolution occurs and cathodic areas where reduction of oxygen occurs. Table 2 shows that the cathodic slopes (βc) changes obviously with the modified of $H_2O_2$. However, the anodic slopes (βa) have similar values. The change of the βc indicated that coated samples decreased the rate of cathodic reaction, because the conversion coatings created a barrier to the supply of oxygen. And the values of βa illustrated that the coatings exerted a weak influence on the anodic reaction. For different coated samples, the cathodic response was more effective in constraining the cathodic reaction for cerium-based conversion coatings on aluminum alloy. Cathodic reaction was suppressed, thereby reducing the driving force of corrosion. Additionally, the addition of $H_2O_2$ could reduce the current density of cerium coated aluminum alloy, and this reduction is pronounced on the cathodic branch but not notable on the anodic branch. According to the literature[14, 23], this phenomenon further justifies the Ce-based coating is the deposition film of insoluble cerium salts on the alloy surface, which covers the cathodic sites. Moreover, it is also found that the specimens treated in the conversion solution with 80mL/L $H_2O_2$ exhibits the best performance of corrosion resistance with an efficiency of 94.03%, as the same change trend as that of corrosion potential. That is, as the concentration of $H_2O_2$ is below 80mL/L, the corrosion current density of coated aluminum alloy decreases with the concentration of additive (Fig.4a), but the current density will increase when the $H_2O_2$ concentration exceeds that value.

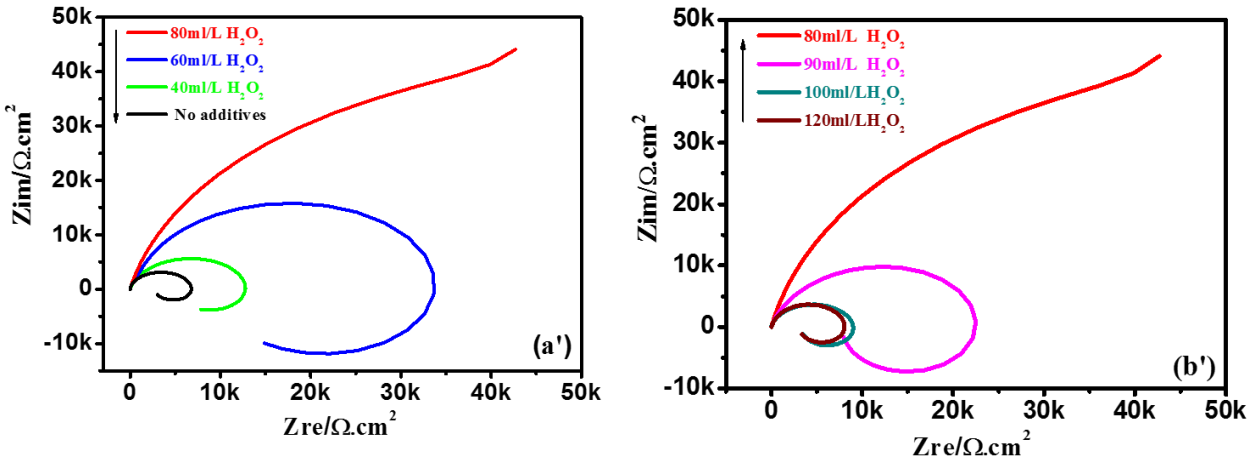


**Figure 5.** Nyquist plots corresponding to the coatings obtained in cerium-based solution for different hydrogen peroxide concentration. (a') The effect of $H_2O_2$ concentration below 80ml/L; (b') The effect of $H_2O_2$ concentration above 80ml/L.

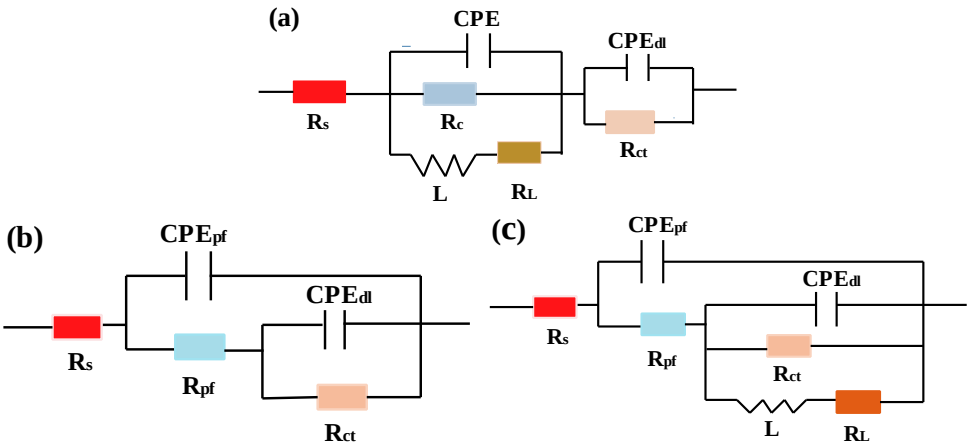


**Figure 6.** (a) The equivalent circuit model used for the bare substrate; (b) Equivalent circuit model used for the alloy treated in cerium-based bath at 25℃ for 20min; and (c) Model proposed to carry out curve fitting of other EIS data from Ce-based treated specimens.

**Table 3** Parts of the fitted electrochemical impedance parameters of Ce-based coatings obtained under different hydrogen peroxide concentration in 3% NaCl solution

| C $H_2O_2$ | $R_s$ ($\Omega cm^2$) | $CPE_{pf}$ $Y_0$($\mu F/cm^2$) | n | $R_{pf}$ ($\Omega \cdot cm^2$) | $R_{ct}$ ($\Omega \cdot cm^2$) | L ($H \cdot cm^2$) |
|---|---|---|---|---|---|---|
| Blank | 1.748 | 13.69 | 0.9344 | 2220 | 942.9 | 7343 |
| No additives | 2.332 | 9.901 | 0.9335 | 2775 | 4130 | 17100 |
| 40ml/L | 1.481 | 9.585 | 0.9120 | 5005 | 8372 | 19510 |
| 60ml/L | 1.985 | 10.85 | 0.9149 | 9530 | 26250 | 91710 |
| 80ml/L | 1.754 | 6.898 | 0.9403 | 92000 | 1.172E5 | — |
| 90ml/L | 1.666 | 12.34 | 0.8834 | 7758 | 18530 | 27520 |
| 100ml/L | 1.459 | 9.312 | 0.9195 | 3234 | 6487 | 17600 |
| 120ml/L | 1.711 | 8.439 | 0.9283 | 3040 | 5142 | 20240 |

We also employed the measurement of electrochemical impedance spectroscopy to further explore the anti-corrosion behavior of the Ce-based coating on the aluminum alloy after treatment in conversion solution with different concentration of $H_2O_2$, as shown in Fig.4a'-b'. Except the one treated with 80ml/L $H_2O_2$, all the other Nyqusit plots show a depressed capacitive loop in the high frequency range and an inductive loop in the low frequency range. The depressed capacitive loop is caused by the geometrical parameters of electrode microstructure[24], which is mainly attributed to the surface roughness or inhomogeneous of conversion coating. As for the inductive loop in the low frequency region, it is an evidence for the occurrence of pitting corrosion on the specimens surface, which suggests the coating would be defective with crevices. However, the Nyquist plot of specimens treated with 80ml/L $H_2O_2$ is characterized with two consecutive capacitive loops, implying that this conversion coating could keep intact in corrosion solution and exhibit the best protection performance, which is good agreement with Tafel test. Besides, we also observed the inhibition efficiency of Ce-based coating increases with the concentration of additive ($H_2O_2$) in the conversion solution when its concentration is lower than 80ml/L, but the inhibition efficiency will decrease at higher concentrations, which also displays the same trend as that obtained with Tafel polarization curves, demonstrating the reliability of our results.

As reported[13, 22, 25, 26], when the aluminum alloy is immersed into cerium salts solution, the galvanic corrosion reaction will occur as follow:

Anodic region: $Al \rightarrow Al^{3+} + 3e^-$ (R1)

Cathodic region: $2H^+ + 2e^- \rightarrow H_2 \uparrow$ (R2)

If $H_2O_2$ is added into the conversion solution, the cathodic reaction will be complemented with following reaction:

$H_2O_2 + 2e^- \rightarrow 2OH^-$ (R3)

Thus, the additive of $H_2O_2$ plays mainly two roles in the coating formation on the aluminum alloy surface. At first, $H_2O_2$ is a strong oxidizing agent, it can oxidize, Ce(Ⅲ) in the conversion solution to Ce(Ⅳ) species, which is much more easy to form insoluble salts on the alloy surface. Secondly, Due to R3, the local pH around cathodic region will be increased, which promotes the reaction of the Ce(Ⅲ) and Ce(Ⅳ) species with $OH^-$ to form insoluble salts of $Ce(OH)_3$ and $Ce(OH)_4$ as coating components. Besides, the oxidizing property of $H_2O_2$ will also accelerate $Ce(OH)_3$ and $Ce(OH)_4$ to $CeO_2$, which is pretty stable in corrosion solution. Thus, the addition of $H_2O_2$ into the conversion solution improved the corrosion resistance of Ce-based coating on the aluminum alloy. However, when the concentration of $H_2O_2$ is at a relative high level exceeding 80mL/L, the deposition rate of insoluble salts is too fast, which forms thick but porous coating on the metal surface. Such coatings will induce lots of crevices during the dehydration process before corrosion test.

### *3.3.2 The effect of immersion time*

In addition to the concentration of additive, the immersion time and the bath temperature are another two critical factors for the performance of conversion coatings. In this section, we evaluate the effect of immersion time at first. Fig. 7 shows the Tafel polarization curves of the ADC12 aluminum

alloy after treatment in cerium salts solution for different immersion time, and the corresponding corrosion parameters are listed in Table 4.

From the polarization curves, we can observe that the specimens treated for 20 mins exhibits the best performance with an efficiency of 94.03%. And also, the corrosion potential ($E_{corr}$) of cerium coated aluminum alloy is also negatively shift and corrosion current density ($I_{corr}$) decreases with immersion time at first (Fig 7a, the immersion time is shorter than 20mins). However the $E_{corr}$ converts to positive shift and the corresponding $I_{corr}$ increase with the immersion time, when the specimens are immersed into the conversion time for longer time (Fig.7b, longer than 20 mins). Besides, the influence of immersion time on the polarization curves is also pronounced on the cathodic branch.

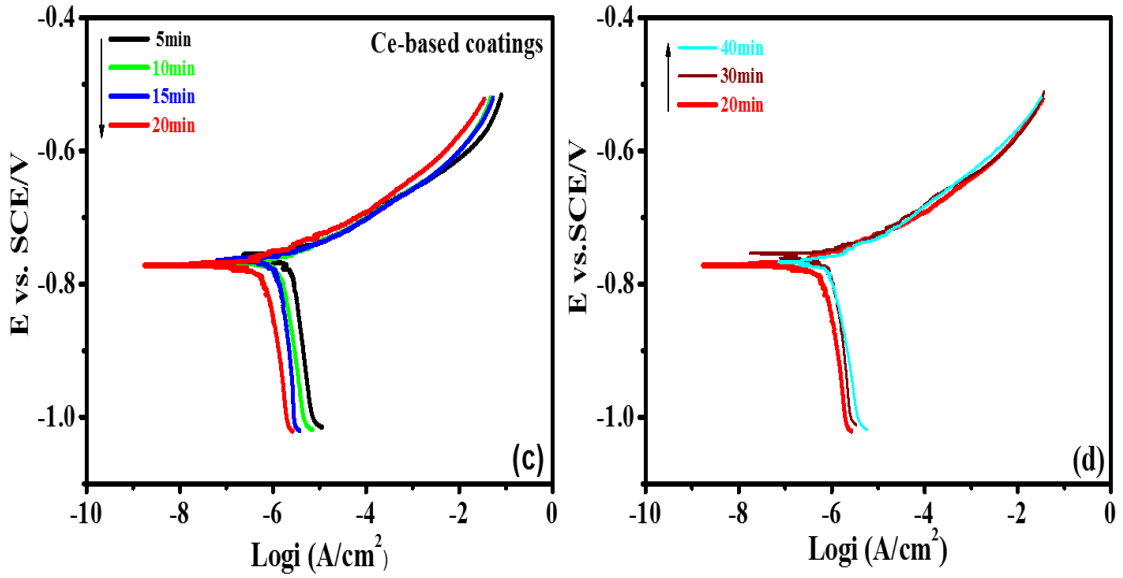


**Figure 7.** Potentiodynamic polarization curves of cerium-coated Al alloy in 3% NaCl solution. (c) The effect of immersion time on polarization curves below 20min; (d) The effect of immersion time on polarization curves above20min; ($Ce(NO_3)_3$=5g/L, $H_2O_2$ =80ml/L, T=25℃).

**Table 4** Potentiodynamic polarization parameters for the corrosion of Cerium-coated aluminum alloy in 3% NaCl solution obtain after different immersion time

| Time (min) | $E_{corr}$ (mV/SCE) | $\beta_c$ ($mV \cdot dec^{-1}$) | $\beta_a$ ($mV \cdot dec^{-1}$) | $I_{corr}$ ($\mu A \cdot cm^{-2}$) | IE (%) |
|---|---|---|---|---|---|
| 5min | -756 | 523.01 | 30.25 | 2.833 | 69.89% |
| 10min | -769 | 428.63 | 36.47 | 2.125 | 77.42% |
| 15min | -764 | 496.77 | 29.71 | 1.493 | 84.13% |
| 20min | -772 | 389.26 | 37.04 | 0.562 | 94.03% |
| 30min | -754 | 421.59 | 28.46 | 1.165 | 87.62% |
| 40min | -767 | 331.79 | 36.13 | 1.254 | 86.67% |

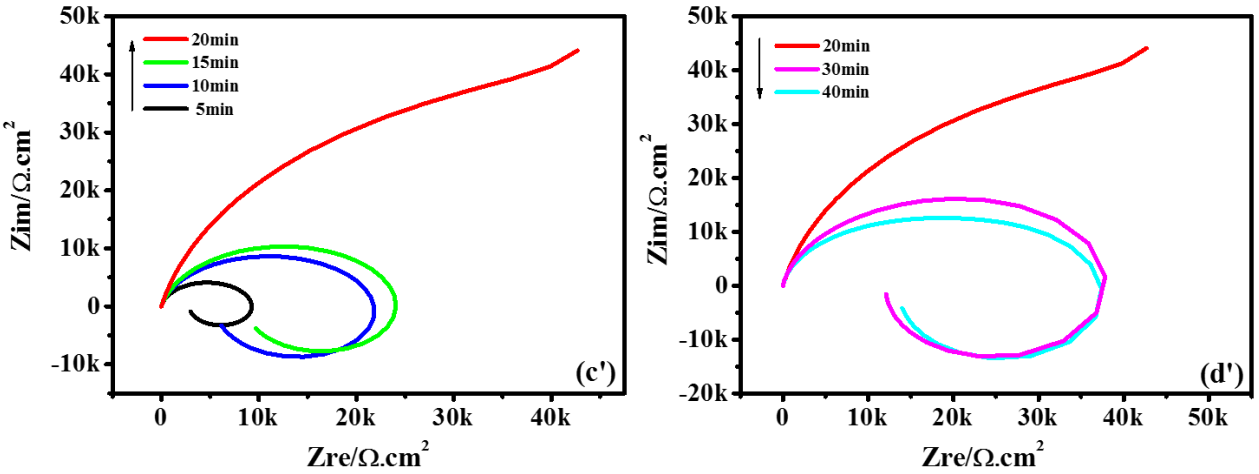


**Figure 8.** Nyquist plots corresponding to the coatings obtained in cerium-based solution for different immersion time. (c') The effect of immersion time below 20min; (d') The effect of immersion time above 20min.

**Table 5** Parts of the fitted electrochemical impedance parameters of Ce-based coatings obtained under different immersion time in 3% NaCl solution

| Time (min) | $R_s$ ($\Omega cm^2$) | $CPE_{pf}$ $Y_0(\mu F/cm^2)$ | n | $R_{pf}$ ($\Omega \cdot cm^2$) | $R_{ct}$ ($\Omega \cdot cm^2$) | L ($H \cdot cm^2$) |
|---|---|---|---|---|---|---|
| 5min | 1.866 | 6.984 | 0.9546 | 2878 | 6736 | 14240 |
| 10min | 1.869 | 7.398 | 0.9146 | 5556 | 11220 | 33270 |
| 15min | 2.006 | 9.205 | 0.9003 | 8707 | 17000 | 64310 |
| 20min | 1.754 | 6.898 | 0.9403 | 92000 | 1.172E5 | — |
| 30min | 1.674 | 7.529 | 0.9271 | 13520 | 76720 | 66400 |
| 40min | 2.223 | 7.384 | 0.9220 | 12050 | 24750 | 25970 |

The results of polarization curves were further confirm with EIS, as shown in Fig.8c'-d'. These EIS plots are also fitting with the equivalent circuit in Fig.1c and their corresponding parameters are listed in Table 2. We can observe that the charge transfer resistance ($R_{ct}$) for corrosion reaction specimen increases with the immersion time at first and reaches the maximum value at 20mins. If the immersion time is extended, the $R_{ct}$ begins to decrease. Additionally, the Nyquist plots of specimen after immersion for 20mins (Red curves in Fig.8c'-d') display two consecutive capacitance loops at the high and the low frequency region, respectively. Such impedance responses indicate that the reaction system is stable during the electrochemical measurement, suggesting that its Ce-based coating could keep intact in the corrosion solution and prevent the attack of aggressive ions. However, the other plots exhibit an inductive loop at the low frequency. This inductive loop is due to the occurrence of pitting corrosion, implying there are crevices on the coatings.

Based on above observation, we find that the optimal immersion time is 20mins, which might be a compromise time for coating formation and coating thickness. If the immersion time is too short, there is no enough time for the insoluble salts depositing on the alloy surface to form coating. But if the time is too long, the coating is very thick. According to Kanani[14], the coating thickness is one key factor for propagation of cracks in it, and the coating strength will decrease as the coating thickness increase. Thus, there emerge more cracks for thinker coating during the dehydration process before corrosion test, leading to the performance decrease of Ce-based coating.

### *3.2.3 The effect of bath temperature*

The effect of bath temperature on the performance of Ce-based coating was also investigated. The Ce-based coating were prepared on the aluminum alloy under different bath temperature, and then, their electrochemical behaviors in 3% NaCl solution were studied. The obtained polarization curves was show in Fig. 9, and their corresponding corrosion parameters are listed in Table 3.

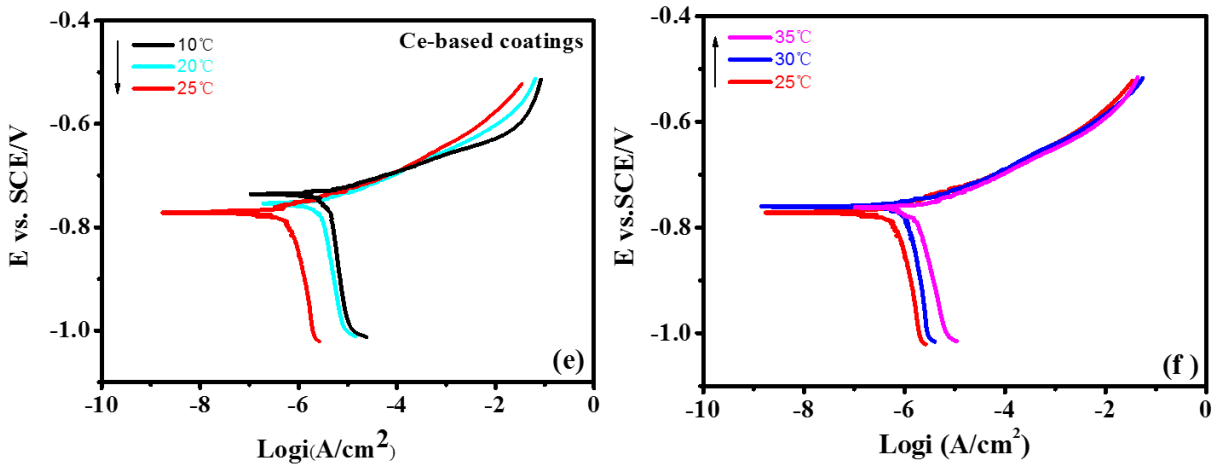


**Figure 9.** Potentiodynamic polarization curves of cerium-coated Al alloy in 3% NaCl solution, (e) The effect of bath temperature on polarization curves below 25℃; (f) The effect of bath temperature on polarization curves above 25℃; ($Ce(NO_3)_3$=5g/L, $H_2O_2$ =80ml/L, t =20min).

**Table 6** Potentiodynamic polarization parameters for the corrosion of Cerium-coated aluminum alloy in 3% NaCl solution obtain after different bath temperature

| T (℃) | $E_{corr}$ (mV/SCE) | $\beta_c$ ($mV \cdot dec^{-1}$) | $\beta_a$ ($mV \cdot dec^{-1}$) | $I_{corr}$ ($\mu A \cdot cm^{-2}$) | IE % |
|---|---|---|---|---|---|
| 10℃ | –736 | 697.84 | 32.07 | 6.001 | 36.22% |
| 20℃ | –754 | 524.11 | 36.78 | 4.797 | 49.02% |
| 25℃ | –772 | 389.26 | 37.04 | 0.562 | 94.03% |
| 30℃ | –760 | 442.09 | 32.94 | 1.255 | 86.66% |
| 35℃ | –762 | 359.84 | 29.20 | 2.871 | 69.49% |

It can be seen that the protection efficiency of Ce-based coatings increase with the bath temperature at first (below 25℃ ) and reach the best performance at 25℃, afterwards, the efficiency decreased with bath temperature (above 25℃). Correspondingly, the $I_{corr}$ decreases at first and reaches the minimum value of 0.562μA · $cm^{-2}$, and then increases to 2.871μA · $cm^{-2}$ at 35℃.

The results of EIS are also in agreement with that of polarization curves. The EIS plots of the samples in 3% NaCl solution after being treated in cerium conversion solution under different bath temperatures in shown in Fig.10e'-f', and the extracted impedance parameters with equivalent circuit in Fig. 6c is listed in Table 7. The Nyquist plots of the sample treated under 25 ℃ is characterized with two consecutive capacitive loops with maximum impedance value, suggesting the Ce-based coating on this specimen has no cracks and exhibits best performance to protect the alloy substrate.

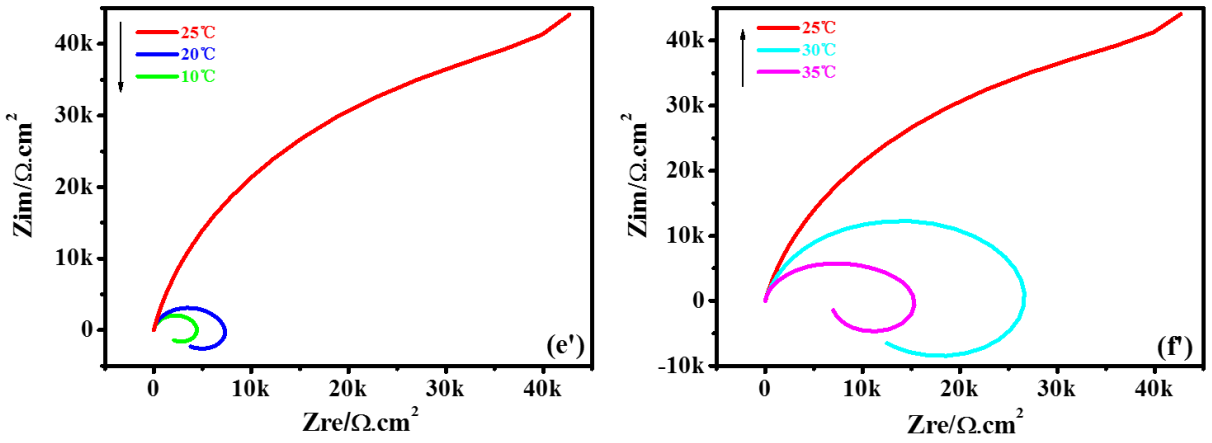


**Figure 10.** Nyquist plots corresponding to the coatings obtained in cerium-based solution for different bath temperature. (e') The effect of temperature below 25℃; (f') The effect of temperature above 25℃.

**Table 7.** Parts of the fitted electrochemical impedance parameters of Ce-based coatings obtained under different temperature in 3% NaCl solution

| T (℃) | $R_s$ (Ω · $cm^2$) | $CPE_{pf}$ $Y_0$(μF/$cm^2$) | n | $R_{coat}$ (Ω · $cm^2$) | $R_{ct}$ (Ω · $cm^2$) | L (H·$cm^2$) |
|---|---|---|---|---|---|---|
| 10℃ | 2.065 | 7.768 | 0.9563 | 1238 | 3190 | 13820 |
| 20℃ | 2.082 | 6.912 | 0.9457 | 2477 | 9881 | 14480 |
| 25℃ | 1.754 | 6.898 | 0.9403 | 92000 | 1.172E5 | — |
| 30℃ | 1.840 | 7.764 | 0.9263 | 9459 | 18180 | 70310 |
| 35℃ | 1.920 | 7.530 | 0.9341 | 6817 | 15910 | 29820 |

Obviously, the bath temperature has dual effects on the coating formation in cerium solution. On the hand, the bath temperature could accelerate ionic transport from bulk solution to the alloy

surface for coating formation, and also promote the growth of conversion coating for better corrosion protection[27]. Therefore, the coating performance increases with the bath temperature at first. On the other hand, the additive of $H_2O_2$ will decompose faster with the increase of bath temperature, which limits its enhancing ability for coating formation, leading the reduction of protection performance at higher bath temperature.

## 4. CONCLUSIONS

The electrochemical behavior and the microstructural features of ADC12 aluminum alloy were investigated in 3%NaCl solution after being treated with cerium conversion condition under different conversion conditions by using potentiodynamic polarization, electrochemical impedance, contact angles and SEM-EDS analysis. The following conclusions can be drawn from these studies:

Tafel plots and EIS measurements indicates that the Ce-based conversion treatment can improve the corrosion resistance of aluminum alloy, and the coating treated in $Ce(NO_3)_3$-$H_2O_2$ solution produced more resistance surface than that of the one treated without $H_2O_2$. Immersion time and bath temperature for the conversion process had an important influence on the corrosion properties and optimum coating performance was obtained by 20min immersion at 25℃. The coating produced for shorter immersion time was not uniform, while the longer immersion time led to some cracks on the surface. The bath temperature has dual effects on the coating formation. Higher temperature could accelerate ionic transport from bulk solution to the alloy surface for coating formation, while $H_2O_2$ will decompose faster, which limits its enhancing ability for coating formation, leading to the reduction of protection performance.

SEM images showed the coating treatment in $Ce(NO_3)_3$-$H_2O_2$ appears to be more even and smoother than that formed without additive. And the EDS analysis reveals that the surface treated in $Ce(NO_3)_3$-$H_2O_2$ solution have higher cerium content. More pits are observed on the surface of the sample treated in cerium nitrate solution and few pits are observed on the surface of the one treated in additive after immersion in 3%NaCl solution for one hour. Contact angle measurements demonstrated that the treatment with additive had better surface hydrophobicity than the one without additive, confirming that the coating treated in $Ce(NO_3)_3$-$H_2O_2$ solution produced more resistant surface than that of the one treated without $H_2O_2$.

ACKNOWLEDGEMENTS
This work was supported by Natural Science Foundation of China (No. 21376282), and Chongqing Innovation Fund for Graduate Students (No. CYB14019).

## Reference

1. K. H. Na, S. I. Pyun, *Corros Sci*., 50 (2008) 248
2. K. Brunelli, F. Bisaglia, J. Kovac, M. Magrini, M. Dabala, *Mater Corros.*, 60 (2009) 514
3. B. Chen, Q. Li, H. Gao, J. M. Fan, X. Tan, *Mater Corros*., 60 (2009) 521
4. C. F. Malfatti, T. L. Menezes, C. Radtke, J. Esteban, F. Ansart, J. P. Bonino, *Mater Corros*., 63

(2012) 819
5. E. P. Banczek, S. R. Moraes, S. L. Assis, I. Costa, A. J. Motheo, *Mater Corros*., 64 (2013) 199
6. E. Darmiani, I. Danaee, M. A. Golozar, M. R. Toroghinejad, *J Alloy Compd*., 552 (2013) 31
7. E. Darmiani, I. Danaee, M. A. Golozar, M. R. Toroghinejad, A. Ashrafi, A. Ahmadi, *Mater Design*, 50 (2013) 497
8. E. Mccafferty, *J Electrochem Soc*., 126 (1979) 385
9. V. Moutarlier, B. Neveu, M. P. Gigandet, *Surf Coat Tech*., 202 (2008) 2052
10. A. S. Hamdy, H. M. Hussien, *Int J Electrochem Sci*., 9 (2014) 2682
11. J. M. Ferreira, J. L. Rossi, M. A. Baker, S. J. Hinder, I. Costa, *Int J Electrochem Sci*., 9 (2014) 1827
12. B. R. W. Hinton, J Alloy Compd, 180 (1992) 15
13. M. Dabala, E. Ramous, M. Magrini, *Mater Corros*., 55 (2004) 381
14. M. Kanani, I. Danaee, M. H. Maddahy, *Mater Corros*., 65 (2014) 1073
15. J. Sun, G. Wang, *Surf Coat Tech*., 254 (2014) 42
16. A. Aballe, M. Bethencourt, F. J. Botana, M. Marcos, *J Alloy Compd*., 323 (2001) 855
17. B. S. Gu, J. H. Liu, *J Rare Earth*, 24 (2006) 89
18. H. Allachi, F. Chaouket, K. Draoui, *J Alloy Compd*., 491 (2010) 223
19. H. W. Shi, F. C. Liu, E. H. Han, *Mater Chem Phys*., 124 (2010) 291
20. H. W. Shi, E. H. Han, F. C. Liu, *Corros Sc*i., 53 (2011) 2374
21. P. Campestrini, H. Terryn, A. Hovestad, J. H. W. de Wit, *Surf Coat Tech*., 176 (2004) 365
22. A. Conde, M. A. Arenas, A. de Frutos, J. de Damborenea, *Electrochim Acta*, 53 (2008) 7760
23. H. Hasannejad, M. Aliofkhazraei, A. Shanaghi, T. Shahrabi, A. R. Sabour, *Thin Solid Films*, 517 (2009) 4792
24. Z. Lukacs, J Electroanal Chem, 432 (1997) 79
25. A. Aballe, M. Bethencourt, F. J. Botana, M. J. Cano, M. Marcos, Mater Corros, 52 (2001) 344
26. M. Dabala, L. Armelao, A. Buchberger, I. Calliari, *Appl Surf Sci*., 172 (2001) 312
27. B. Y. Johnson, J. Edington, M. J. O'Keefe, *Mat Sci Eng a-Struct.*, 361 (2003) 225